THE THERMODYNAMIC PROPERTIES OF SOLID AND FLUID HELIUM-3 AND HELIUM-4 ABOVE 3 °K AT HIGH DENSITIES

By J. S. DUGDALE and J. P. FRANCK†

Division of Pure Physics, National Research Council, Ottawa, Canada

(*Communicated by G. Herzberg, F.R.S.—Received* 14 *October* 1963)

CONTENTS

Measurements have been made of the specific heat at constant volume of solid ^{3}He from 3 °K up to the melting point at a number of different densities corresponding to pressures up to 2000 atm. The measurements have been extended through the melting region at constant volume up to 29 °K in the fluid phase. For comparison similar measurements have been made on ^{4}He at four different densities.

By combining these data with the p-V-T data of Mills & Grilly (1955) and Grilly & Mills (1959), the complete thermodynamic properties of the solids have been derived in the relevant pressure and temperature range. The results can be understood semi-quantitatively in terms of the zero-point energy of the solids and a quasi-harmonic model of the lattice vibrations. A brief discussion of the specific heat of the fluid phase is also given.

1. Introduction

Simon (1934) first drew attention to the importance of zero-point energy in interpreting the properties of solid and liquid helium. If helium behaved classically, it would exist as a solid in equilibrium with its vapour at the lowest temperatures with a molar volume of about 10 cm^3 and a latent heat of sublimation of about 150 cal/mole; all this can be readily deduced from the properties of the gas phase at higher temperatures. In fact experiment shows that solid ^{4}He is *not* in equilibrium with the vapour phase at *any* temperature and that at the lowest temperatures it exists in equilibrium with the liquid under a pressure of about 25 atm. Its molar volume under these conditions is more than 20 cm^3 and its internal energy

† Now at the Department of Physics, University of Alberta, Edmonton, Canada.

Phil. Trans. Roy. Soc. London
Vol. 257. A. 1076. (Price 10*s*. 6*d*.; U.S. $1.55) 1 [Published 19 November 1964

with respect to the gas phase (infinitely dispersed) is only 12 cal/mole. These differences between the actual behaviour and that of the classical model are due to zero-point energy.†

A similar situation occurs in ^{3}He although, since the atomic mass is smaller and the interatomic potential the same, the zero-point energy has an even greater influence here. In addition to the mass difference, the nucleus of ^{3}He has a spin value of $\frac{1}{2}$ while that of ^{4}He has no spin. This has important consequences for the relative entropies of the liquid and solid phases of ^{3}He at low temperatures and leads to a minimum in the melting curve of ^{3}He at about 0·3 °K. In this paper we are concerned with the solid phase region above

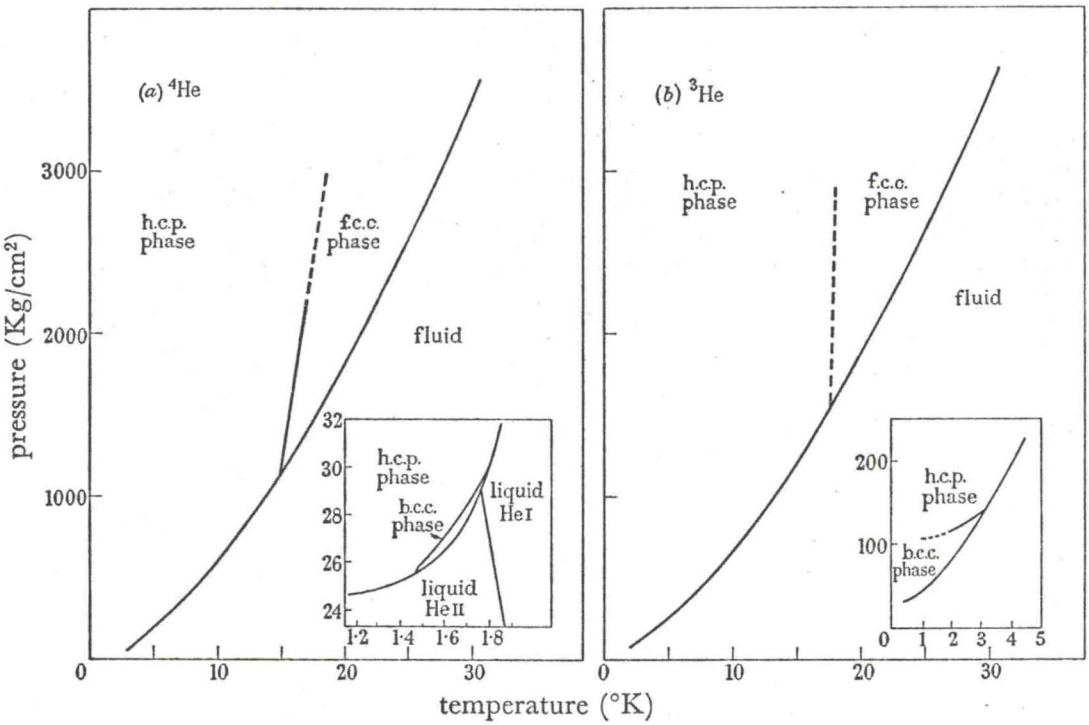

FIGURE 1. (*a*) Phase diagram of ^{4}He. (*b*) Phase diagram of ^{3}He.

about 3 °K and at pressures less than about 2000 atm. In this region, it appears that the nuclear spins are randomly oriented so that there is an additional entropy of $R \ln 2$ which is absent in ^{4}He (cf. the end of § 3·1 below). This spin difference is also associated with a difference in the statistics appropriate to the two isotopes and this shows up very remarkably in the very different properties of the two liquid isotopes. (For a review of the properties of solid and liquid ^{3}He see, for example, Bernardes & Brewer 1962.)

In both the solid isotopes of helium there exist at least three different structures, body-centred cubic, hexagonal close-packed and face-centred cubic. The phase diagram for both solid isotopes is shown in figure 1. According to classical lattice theory, a solid composed of atoms which have central, additive short-range forces should have a close-packed structure. In helium where the condition of central, additive short-range forces between atoms should be realized, we might therefore expect to find either of the two close-packed structures: on the other hand, the existence of the b.c.c. structure is unexpected. Almost certainly this is another illustration of the influence of zero-point energy.

† For a review of work on solid ^{4}He up to 1956 see, for example, Domb & Dugdale (1957).

The experiments which we shall now describe were designed to measure the specific heat at constant volume of solid ^{3}He at temperatures from about 3 °K up to the melting point at different densities corresponding to pressures up to 2000 atm. The melting region at constant volume was also investigated and measurements were made in the fluid region up to 29 °K. The general scope of the experiments was similar to that of the experiments by Dugdale & Simon (1953) on solid ^{4}He. For comparison with these experiments and because the present apparatus is capable of higher accuracy than that of the earlier work, we have made some measurements on ^{4}He. The apparatus and experimental results will now be described.

2. Experimental

2·1. *The calorimeter*

The measurements were made with an adiabatic calorimeter of conventional design. Figure 2 gives a sketch of the calorimeter and the adiabatic shield. The calorimeter incorporates the high pressure cell *A* (which accommodates the helium sample), a gas thermometer bulb *B*, a vapour pressure chamber *C*, a heater *D*, and a thermometer *E*.

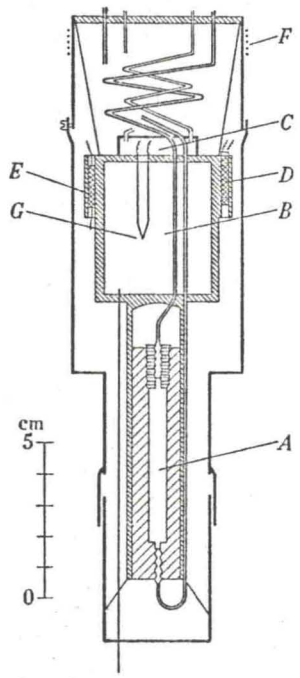

Figure 2. Calorimeter assembly and adiabatic shield.

The pressure cell was machined from a solid cylinder of drillrod steel of $\frac{5}{8}$ in. outer diameter. A hole of $\frac{1}{4}$ in. diameter was drilled to within $\frac{1}{2}$ in. of one end. The opposite end was closed with a threaded plug which was put into place with hard solder. At each end a high pressure steel capillary of 1 mm outside diameter and 0·1 mm bore joined the cell. The capillaries widened at the end to about $\frac{1}{8}$ in. outside diameter and were threaded along this part. The capillaries were then threaded with hard solder into the cell. This technique gives a perfect seal which withstands high pressures. One of the capillaries leads to the filling line whereas the second capillary leads to a small Bourdon gauge.

The gas thermometer bulb was made from copper of $\frac{1}{16}$ in. wall thickness and had a volume of about 33 cm^3. A split copper tube of $\frac{1}{16}$ in. wall thickness extended from the

bottom of the gas thermometer bulb. The pressure cell was placed inside this tube with soft solder. Near the top rim of the gas thermometer bulb several cavities were provided for housing the heater and the thermometer. The gas thermometer bulb, and the receptacles for heater, thermometer, and pressure cell were machined from one piece. This ensured good thermal conduction throughout. The relative positions of heater, thermometer, and pressure cell were so chosen as to avoid any disturbance of the heater or thermometer when the pressure cell was subjected to pressure.

The thermometer is described in § 2·2. The heater consisted of about 2000 Ω of manganin wire, wound on a small copper former which in turn was put with soft solder into one of the cavities. The lead wires for thermometer and heater were lacquered for a length of several centimetres to the calorimeter before leaving it. The lead wires were 36-gauge manganin wire between calorimeter and the liquid helium stage of the cryostat. From there on 34-gauge copper wire was used. The lead wires were brought into thermal contact with the adiabatic shield for about 30 cm. One of the potential leads of the heater was connected at the calorimeter, the other at the adiabatic shield.

The vapour pressure chamber had a volume of about 3 cm^3 and was placed on top of the gas thermometer bulb (figure 2). It is connected to two thin-wall cupro-nickel capillaries of 0·5 mm bore. Both capillaries as well as the high pressure capillaries leading to the pressure cell were wound into spirals 25 cm long before making thermal contact with the adiabatic shield. The gas thermometer bulb was connected to the outside through a thin wall cupro-nickel capillary of 0·3 mm bore; this capillary was brought out through the bottom of the adiabatic shield and the cryostat in order to keep the low temperature part of it as short as possible.

The cryostat contained a stage for liquid hydrogen and a stage for liquid helium. The high-pressure capillaries were thermally anchored for about 50 cm to the liquid helium stage. Under the pressures employed in this investigation the high pressure capillaries were therefore blocked by a plug of solid helium. This made it possible to measure the specific heat at virtually constant volume. The adiabatic shield had a heater of about 1000 Ω at F (figure 2). A differential thermocouple G (silver, 0·37 at. % gold/gold, 2·1 at.% cobalt) indicated the temperature difference between shield and calorimeter. The temperature of the shield was controlled semi-automatically so that the drift of the calorimeter was zero. The calorimeter was cooled to 20 °K by means of exchange gas. The exchange gas was then pumped off and further cooling was achieved by passing cold helium gas through the vapour pressure chamber. The lowest temperatures were obtained by liquefying some helium (^{4}He) in the vapour pressure chamber and then pumping it off. Measurements were started after a vacuum better than 5×10^{-6} mmHg was established in the vacuum line connected to the vapour pressure chamber for about 10 min.

The heat capacity measurements were made in the usual way. Heating intervals varied from about 0·06 deg near 3 °K to 0·6 deg near 30 °K. Measurements below about 3 °K were not feasible because the control of the shield temperature became increasingly difficult owing to the reduced sensitivity of the differential thermocouple.

2·2. *Temperature scale*

The thermometer was a 10 Ω, 1 W, Allen–Bradley carbon resistor; its plastic cover was ground off and the resistor then placed inside its cavity with varnish. It was calibrated against the vapour pressures of helium (^{4}He) and hydrogen (of known ortho-para composition) close to their normal boiling points. For interpolation the two-constant formula (Clement 1955) was used,

$$\left(\frac{\log R}{T_c}\right)^{\frac{1}{2}} = a + b \log R, \tag{1}$$

where R is the resistance and the constants a and b are determined from the calibration points. Temperatures as determined from equation (1) are for clarity designated by T_c.

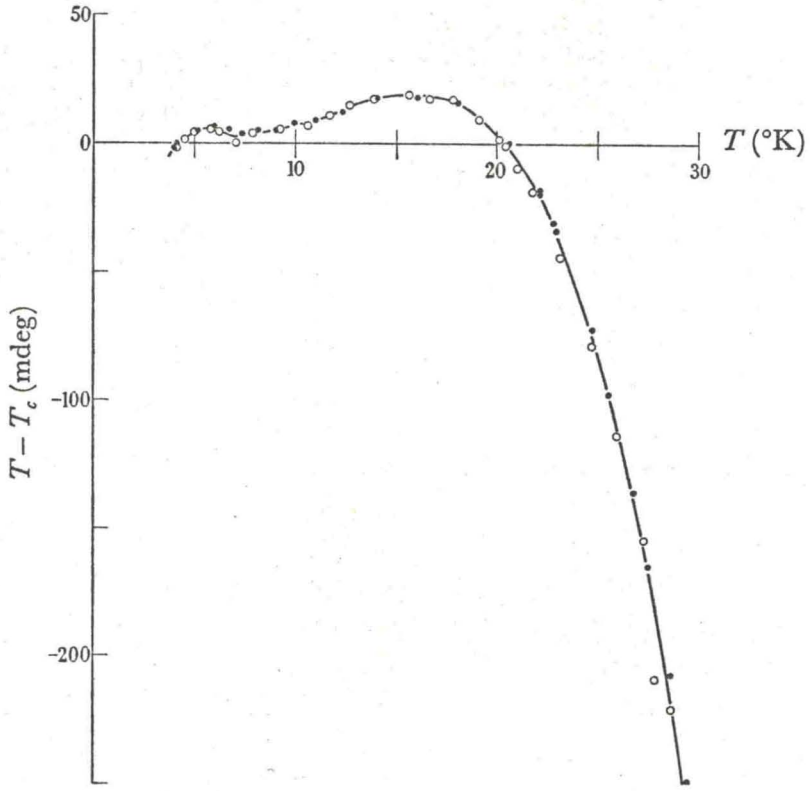

FIGURE 3. Corrections applied to the carbon thermometer temperature T_c to convert it to the absolute temperature T.

This calibration was performed each time after the thermometer had been allowed to warm up to room temperature and a slight change of the constants a and b was observed after each warm-up.

It is known that interpolation with equation (1) leads to serious deviations from true temperature, especially above 20 °K. A complete calibration of the thermometer against the helium gas thermometer was therefore obtained. The technique employed was as described by Franck & Martin (1961). Temperatures as obtained from the gas thermometer readings are designated T and are believed to be accurate to within ±5 mdeg. The results of two calibrations are given in figure 3 as $T-T_c$ plotted against T.

From previous experience with thermometers of the Allen–Bradley type it was known that the effect of successive warm-ups on the deviation curve $T-T_c$ is almost negligible

although the constants a and b may change. The correction $T-T_c$ for all heat capacity measurements was therefore taken from the smoothed curve in figure 3. The temperatures T obtained in this way are estimated to be accurate to within ± 5 mdeg.

2·3. *Gas handling and operation*

A general scheme of the gas handling system is given in figure 4. Different methods were used for handling the two isotopes, because the rare isotope, ^{3}He, had to be recovered completely and was supplied at about atmospheric pressure.

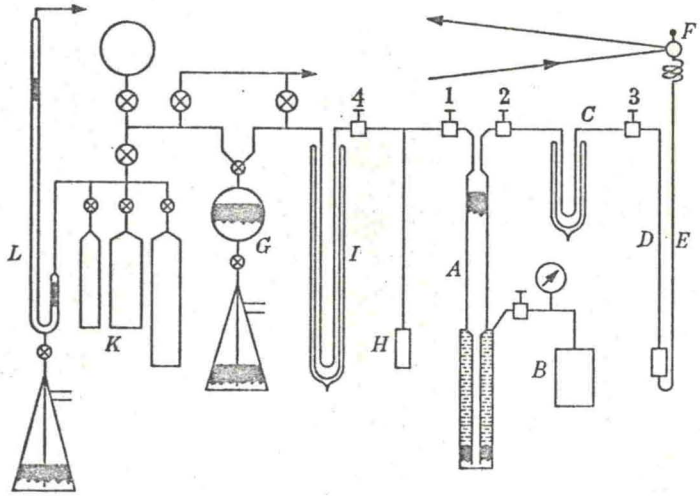

FIGURE 4. Schematic diagram of the gas handling assembly.

^{4}He was taken from a cylinder of commercial helium, purity 99·995 % with the remainder mainly N_2 and CO_2. It was passed at cylinder pressure (*ca.* 150 atm) through a silica-gel trap and a charcoal trap at liquid nitrogen temperature and then fed into the high pressure Toepler pump A. Valve 1 was then closed and the gas pressurized by means of the hydraulic pump B. The gas was fed into the calorimeter through the capillaries C and D of 0·1 mm bore with valves 2 and 3 open. The capillary C passed through liquid nitrogen for about 50 cm. The calorimeter was cooled to 20 °K with valve 3 closed. At 20 °K additional helium was fed into the calorimeter to roughly the required density. The liquid helium stage of the cryostat was then cooled to 4 °K and the calorimeter cooled to below the freezing point with valves 2 and 3 open. No particular care was taken to freeze the sample slowly. Valve 3 was then closed and the measurements started. Valve 3 is a miniaturized high-pressure valve, and care had been taken to avoid dead space. Its dead space on the calorimeter side, when closed, is about 0·0018 cm^3. Pressure transmission to the calorimeter during the filling operation could be easily monitored on the Bourdon gauge F. This gauge was made from copper-beryllium tubing of 0·4 mm bore and had a volume of 0·058 cm^3. Observation of this gauge showed too that the high pressure capillaries D and E stayed blocked while working in the melting and the fluid range.

^{3}He was supplied through the Monsanto Company and the supplied analysis shows no detectable ^{4}He impurity. The gas was pressurized to about 1·5 atm in the low pressure Toepler pump G and condensed under this pressure at about 1·5 °K in the pressure

vessel *H*. Before entering *H* the gas passed through the cold trap *I* at 4 °K. After most of the gas was transferred into *H*, valve 4 was closed and the gas allowed to warm up and enter the high pressure Toepler pump. From this stage on the procedure was the same as with ^{4}He. Before filling with the gas the calorimeter and high pressure Toepler pump had to be evacuated. In the case of ^{4}He the system was pumped for 3 days and then flushed several times at pressures up to 2000 atm with clean ^{4}He. In the case of ^{3}He this method could not be followed. The system was therefore first thoroughly flushed with hydrogen in order to avoid contamination with ^{4}He and then pumped for 11 days. From tests with ^{4}He and a helium leak detector, this time was known to be sufficient to empty the system adequately.

2·4. *Determination of molar volume and mass of sample*

The molar volume of the helium samples was not determined directly but inferred from the melting data of Mills & Grilly (1955), and Grilly & Mills (1959). As the samples were held at constant volume melting took place over a finite temperature interval. The temperature at the beginning of the melting range, T_m, was obtained by taking heating curves. A well pronounced kink in the curve of temperature against time was observed which allowed T_m to be estimated to within 0·002 degK. From this temperature the pressure at the beginning of melting, p_m, and the molar volume V could be calculated using the data of Mills & Grilly.

For the measurements on ^{4}He the mass of the sample was obtained in the following way. After completion of the heat capacity measurements the high-pressure Toepler pump was disconnected at valve 3 (figure 4) and the low-pressure Toepler pump connected to this valve. The gas filling the calorimeter and the dead space up to valve 3 was then transferred quantitatively by means of the Toepler pump to a stack of calibrated volumes *K*. The volumes *K* (roughly 0·6, 1·2 and 2·4 l.) had been calibrated by weighing with water. They were immersed in a water bath whose temperature could be determined to about 0·01 degK. The pressure in *K* was read on the constant volume manometer *L* to better than 0·1 mm using a cathetometer. The mass of helium gas was determined from the *p*-*V*-*T* data given by Keesom (1942) after due corrections for dead space had been applied. The dead space consists of the two high-pressure capillaries *D* and *E* (0·016 cm^3), the Bourdon gauge *F* (0·058 cm^3), and the calorimeter side of the closed valve 3 (0·0018 cm^3). The whole dead space correction is approximately 2·3 % and is estimated to be known to better than 15 %. The accuracy of the mass determination is estimated at 0·5 %.

From the mass determination and the molar volume *V*, the volume *v* of the high-pressure cell could be calculated. The results for *v* (about 1·46 cm^3) obtained in this way showed a slightly increasing cell volume with increasing pressure which agreed with the elastic data for drill rod steel. The average deviation of *v* found in the four ^{4}He experiments from a straight line is 0·2 %.

In the case of ^{3}He it was not thought feasible to transfer the cell content after each measurement to the calibrated volumes. The mass of the samples was instead calculated from the molar volume *V*, obtained as described above, and the cell volume *v*, obtained from the measurements on ^{4}He as described.

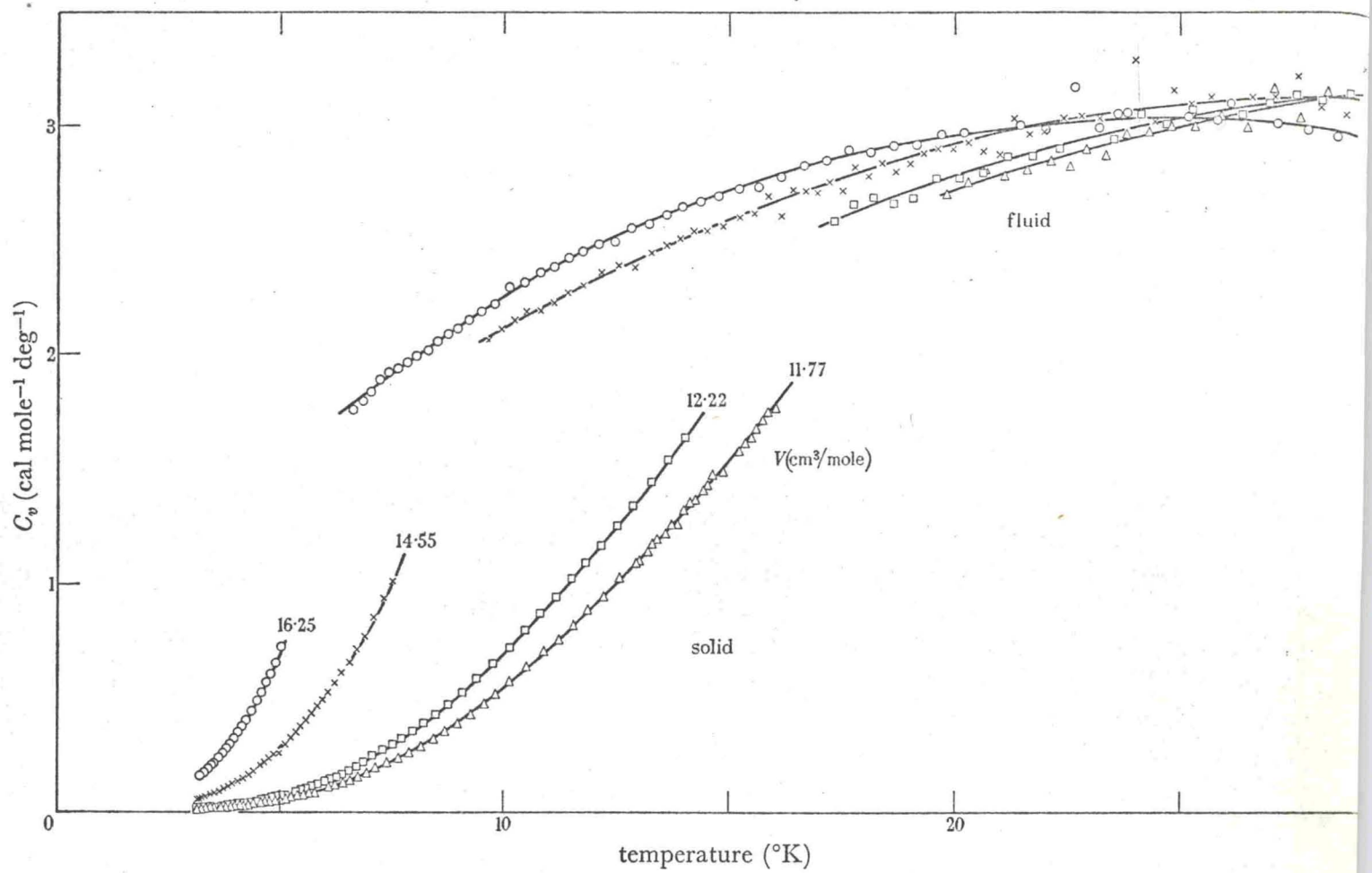

FIGURE 5. The specific heat at constant volume of solid and fluid ^{4}He at various volumes.

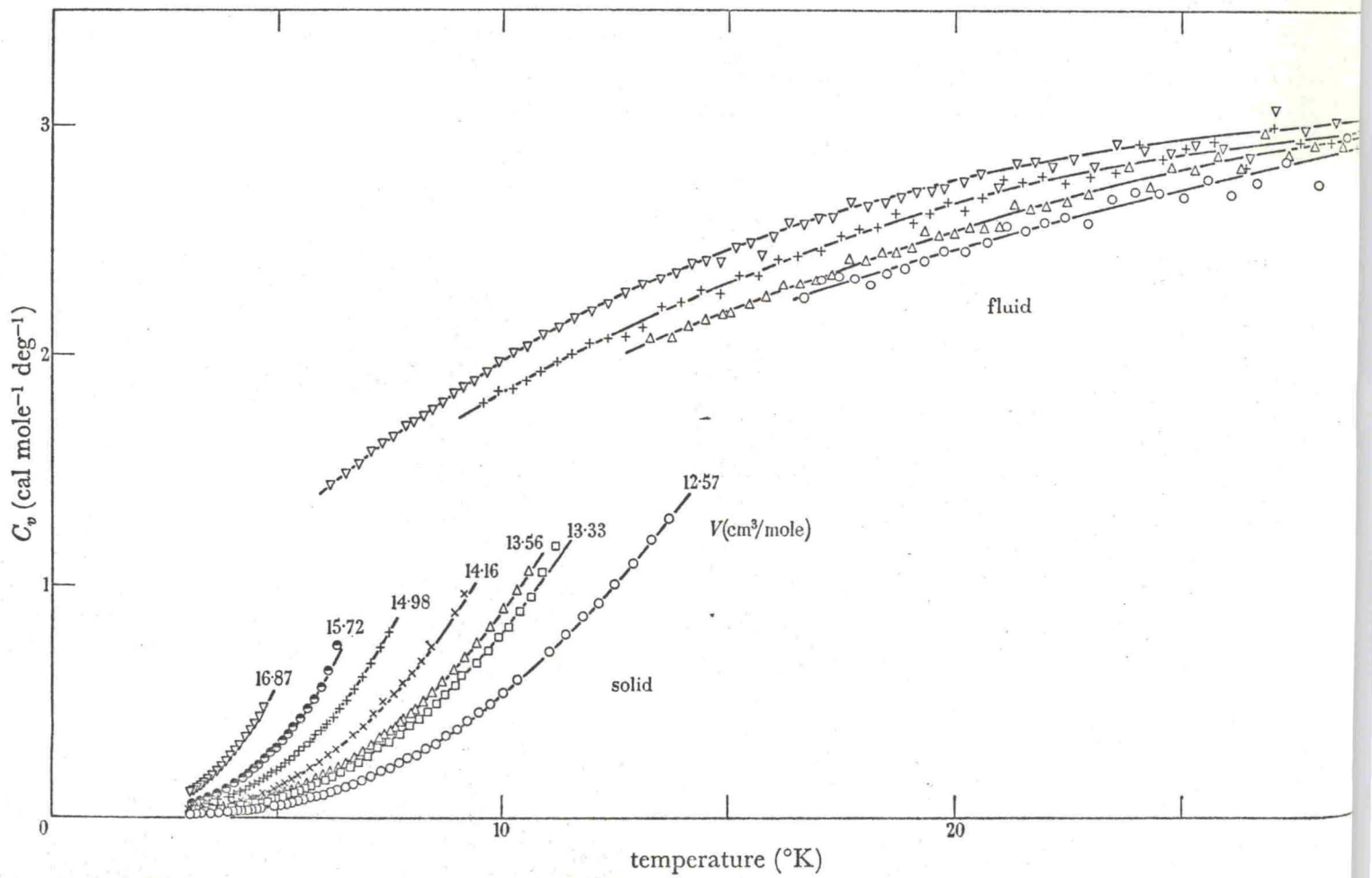

FIGURE 6. The specific heat at constant volume of solid and fluid ^{3}He at various volumes.

3. Experimental results

3·1. *Specific heat of solid helium*

The specific heat of solid ^{4}He was measured at four different molar volumes, and of solid ^{3}He at ten different molar volumes. The results are shown in figures 5 and 6. Debye temperatures θ_D were calculated from the experimental points and are shown in figures 7 and 8. Included in figure 7 are earlier measurements by Keesom & Keesom (1936).

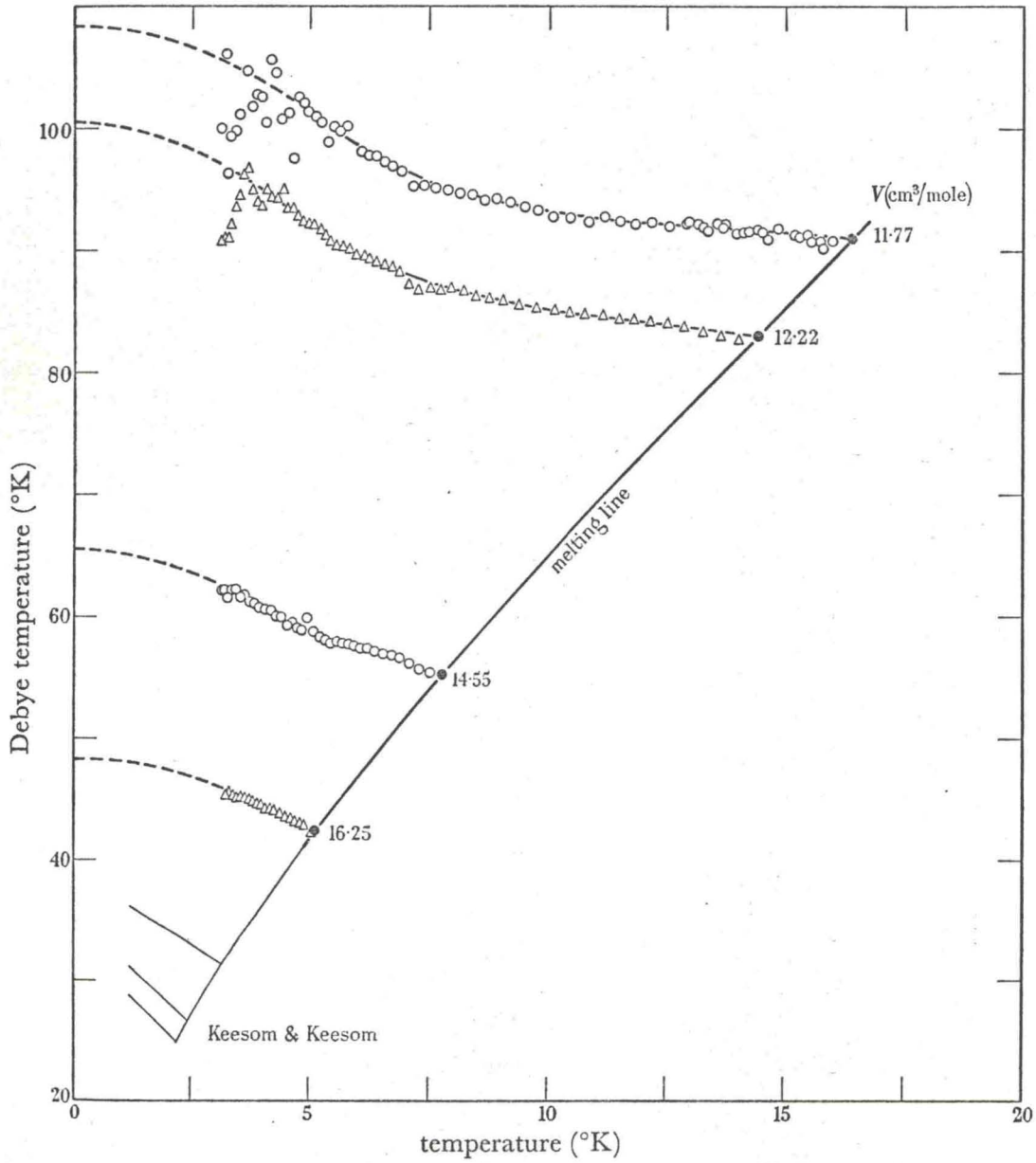

Figure 7. The Debye temperature of solid ^{4}He as a function of temperature at different molar volumes.

The heat capacity of the helium samples contributed from 30 to 40 % of the total measured heat capacity near the melting point. This ratio became progressively worse with falling temperature and varied from 5 to 25 % at 3 °K. The accuracy is therefore greatly reduced below about 5 °K, especially for samples of low molar volume. Because of this we feel that

the apparent decrease of θ_D at the low temperature end of the measurements is probably due to experimental error. Above 5 °K we have about 1 % scatter in C_v. An error of about 0·5 % has to be assigned to the determination of the sample mass. We therefore estimate the error in C_v above 5 °K at about 1·5 %.

In tabulating the results we have proceeded as follows. Smoothed lines were drawn through the plot of Debye temperatures θ_D against T and extrapolated from about 5 to 0 °K

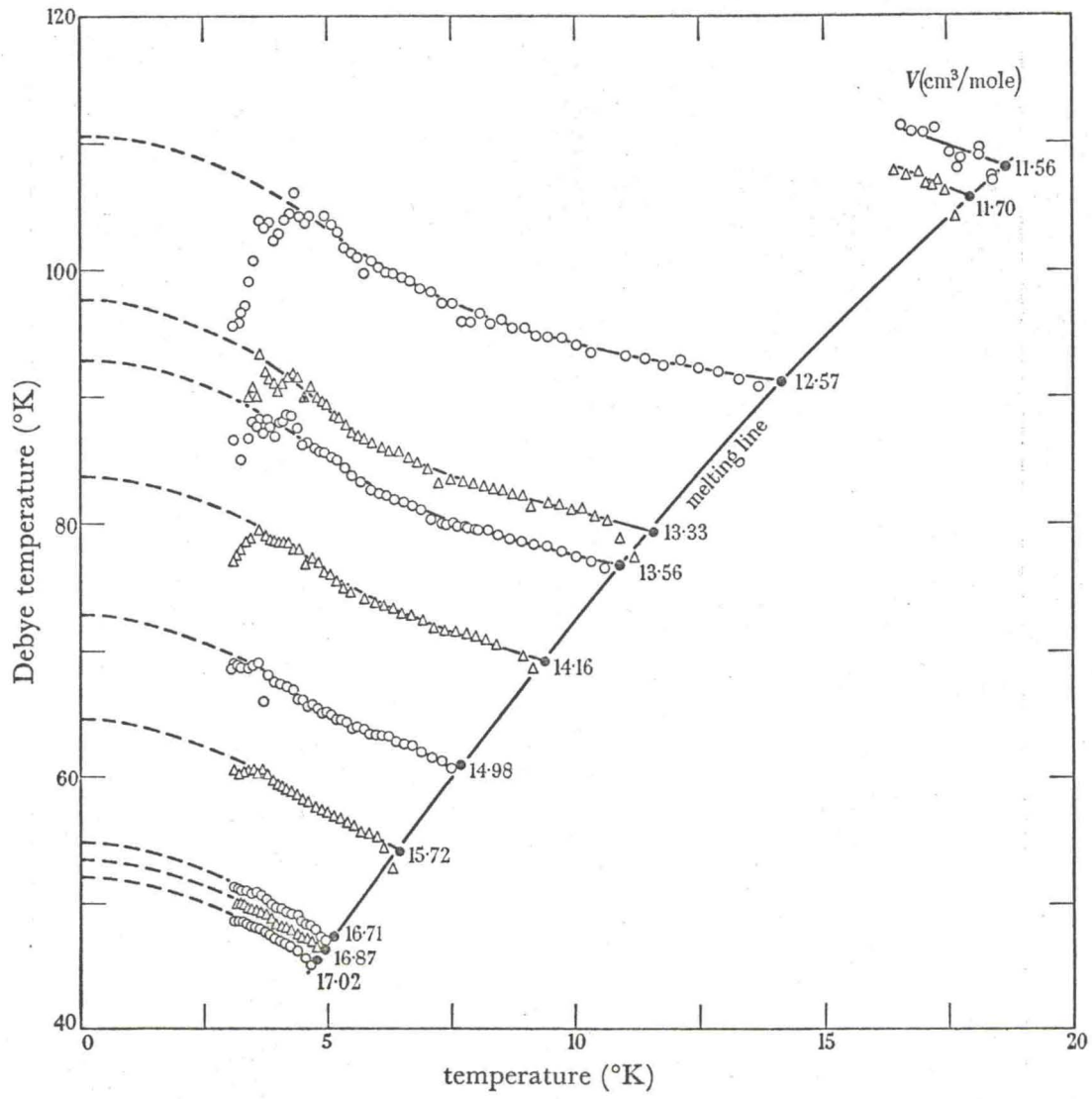

FIGURE 8. The Debye temperature of solid ^{3}He as a function of temperature at different molar volumes.

along the dashed lines. This extrapolation is at present very tentative and is discussed more fully in § 4·1 together with the recent measurements of Heltemes & Swenson (1961, 1962). Values of the specific heat C_v were calculated from the smoothed θ_D plot above 3 °K at rounded values of temperature and are given in tables 1 and 2. It can be seen in figures 7 and 8 that close to the melting point the Debye temperatures tend to be low for some runs. This was attributed to pre-melting phenomena and depends probably on the method of freezing the sample. We have therefore extrapolated the θ_D plot smoothly towards the

temperature of onset of melting. The corresponding values of C_v obtained in this way are tabulated for the actual molar volumes investigated in tables 1 and 2.

The earlier measurements of Dugdale & Simon (1953) agree with the present results to within 2% of C_v near the melting line. With falling temperatures Dugdale & Simon's results become progressively larger than the present ones and at 5 °K the discrepancy in C_v is about 15%. Their measurements did not show the marked rise in θ_D with falling temperature observed here; this rise is, however, in agreement with the results of Keesom & Keesom (1936) at higher molar volumes.

TABLE 1. THERMODYNAMIC FUNCTIONS FOR SOLID ^{4}He AT ROUNDED VALUES OF TEMPERATURE

	V = 16·25			14·55			12·22			11·77		
T (°K)	C_v	$U-U_0$	S	C_v	$U-U_0$	S	C_v	$U-U_0$	S	C_v	$U-U_0$	S
3	0·128	0·0914	0·040	0·0506	0·0363	0·0160	0·0136	0·0099	0·0044	0·0106	0·0077	0·0034
4	0·333	0·310	0·102	0·132	0·123	0·0404	0·0348	0·0328	0·0108	0·0265	0·0254	0·0084
5	0·697	0·811	0·212	0·279	0·322	0·0842	0·0742	0·0855	0·0224	0·0559	0·0652	0·0172
6	—	—	—	0·507	0·708	0·154	0·138	0·189	0·0412	0·105	0·144	0·0313
7	—	—	—	0·816	1·36	0·254	0·232	0·372	0·0692	0·177	0·282	0·0525
8	—	—	—	—	—	—	0·358	0·665	0·108	0·275	0·506	0·0823
9	—	—	—	—	—	—	0·515	1·10	0·159	0·399	0·840	0·122
10	—	—	—	—	—	—	0·700	1·70	0·223	0·549	1·31	0·171
11	—	—	—	—	—	—	0·907	2·50	0·299	0·721	1·95	0·231
12	—	—	—	—	—	—	1·13	3·52	0·387	0·909	2·76	0·302
13	—	—	—	—	—	—	1·37	4·77	0·487	1·11	3·77	0·383
14	—	—	—	—	—	—	1·61	6·26	0·597	1·32	4·98	0·472
15	—	—	—	—	—	—	—	—	—	1·53	6·40	0·571
16	—	—	—	—	—	—	—	—	—	1·75	8·04	0·676

Units: V (cm^3/mole); C_v (cal mole^{-1} deg^{-1}); $U-U_0$ (cal/mole); S (cal mole^{-1} deg^{-1}).

Heltemes & Swenson (1961, 1962) have made measurements on solid ^{3}He and ^{4}He over a range of densities similar to those studied by us but at temperatures between 0·3 and about 1·5 °K. Their results will be discussed more fully in § 4·1 below. At this point it is sufficient to note that they found no evidence of any specific heat anomaly which could be attributed to the nuclear spins in ^{3}He. If the nuclear spins were interacting appreciably one would expect to see an anomaly in the specific heat corresponding to the decrease in entropy from $R\ln 2$ towards zero as the temperature falls. At the high temperature side of such an anomaly the specific heat from this source would be expected to vary as $1/T^2$. Since no such term was detected we shall assume that in solid ^{3}He the spins contribute their maximum entropy ($R\ln 2$) at all the temperatures and densities which concern us here.

3·2. *The melting range*

Melting of the helium samples took place over a finite temperature interval since the volume was kept constant. Within the melting range the measured apparent specific heat depends on the specific heat of the solid and of the fluid, and on the latent heat of melting. The thermal relaxation time is much longer in this range than either in the solid or in the fluid range and it increases considerably towards the high temperature end of the melting range. This is probably due to the fact that the large latent heat of melting has to be transferred through the poorly conducting liquid. Equilibrium times of up to 20 min were

TABLE 2. THERMODYNAMIC FUNCTIONS FOR SOLID ^{3}He AT ROUNDED VALUES OF TEMPERATURE

	V = 17·02			16·87			16·71			15·72			14·98		
T (°K)	C_v	$U-U_0$	S	C_v	$U-U_0$	S	C_v	$U-U_0$	S	C_v	$U-U_0$	S	C_v	$U-U_0$	S
3	0·105	0·0746	0·0328	0·0962	0·0679	0·0298	0·0905	0·0647	0·0285	0·0537	0·0384	0·0169	0·0369	0·0265	0·0117
4	0·281	0·269	0·0843	0·260	0·236	0·0770	0·240	0·221	0·0724	0·142	0·131	0·0429	0·0966	0·0896	0·0294
5	—	—	—	—	—	—	0·526	0·591	0·154	0·307	0·347	0·0906	0·208	0·216	0·0619
6	—	—	—	—	—	—	—	—	—	0·571	0·777	0·168	0·386	0·528	0·115
7	—	—	—	—	—	—	—	—	—	—	—	—	0·636	1·03	0·192
	14·16			14·11			13·56			13·33			12·57		
	C_v	$U-U_0$	S	C_v	$U-U_0$	S	C_v	$U-U_0$	S	C_v	$U-U_0$	S	C_v	$U-U_0$	S
3	0·0237	0·0171	0·0076	0·0226	0·0163	0·0072	0·0172	0·0125	0·0055	0·0149	0·0108	0·0048	0·0100	0·0072	0·0032
4	0·0608	0·0571	0·0188	0·0588	0·0548	0·0180	0·0437	0·0414	0·0137	0·0381	0·0359	0·0118	0·0250	0·0239	0·0079
5	0·131	0·150	0·0392	0·128	0·145	0·0379	0·0937	0·108	0·0282	0·0822	0·0938	0·0246	0·0527	0·0615	0·0162
6	0·247	0·335	0·0726	0·242	0·327	0·0707	0·176	0·240	0·0521	0·156	0·210	0·0456	0·0988	0·136	0·0296
7	0·414	0·661	0·123	0·402	0·645	0·119	0·298	0·474	0·0879	0·262	0·416	0·0771	0·168	0·267	0·0497
8	0·633	1·18	0·192	0·611	1·15	0·186	0·460	0·849	0·138	0·405	0·747	0·121	0·262	0·480	0·0779
9	0·897	1·94	0·281	0·866	1·88	0·272	0·657	1·40	0·203	0·584	1·24	0·179	0·384	0·807	0·116
10	—	—	—	—	—	—	0·888	2·17	0·284	0·798	1·93	0·251	0·533	1·26	0·164
11	—	—	—	—	—	—	—	—	—	1·04	2·84	0·338	0·697	1·88	0·222
12	—	—	—	—	—	—	—	—	—	—	—	—	0·902	2·68	0·292
13	—	—	—	—	—	—	—	—	—	—	—	—	1·11	3·68	0·372
14	—	—	—	—	—	—	—	—	—	—	—	—	1·33	4·91	0·462

Units: V (cm^3/mole); C_v (cal mole^{-1} deg^{-1}); $U-U_0$ (cal/mole); S (cal mole^{-1} deg^{-1}).

observed. Because of this effect the accuracy in this range is reduced and is not better than a few parts per cent.

As already described in § 2·4, the *starting* temperature of the melting range could be obtained by taking heating curves. Because of the extremely large thermal relaxation time near the end of the melting range this method was not feasible to determine the temperature of the *end* of the melting range. This temperature, however, could be calculated in an obvious way from an apparent specific heat measured over a heating interval that included the end of the melting range and part of the fluid range. This method when used for the determination of the temperature of the start of the melting interval gave agreement with the more direct observation from heating curves to within 0·002 degK on the average.

The experimental results of the apparent specific heat in the melting range were used to calculate the change in internal energy and in entropy over the melting range and are dealt with in § 3·5.

3·3. *The high-temperature phase transformation in solid* ^{4}He *and* ^{3}He

Both helium isotopes exhibit at high pressures a phase transition from a hexagonal close-packed to a face-centred cubic structure (Dugdale & Simon 1953; Mills & Schuch 1961; Schuch & Mills 1961). In the course of the present investigation this transition was observed at one molar volume in ^{4}He and at two molar volumes in ^{3}He. A preliminary account of the results on ^{3}He has been already given elsewhere (Franck 1961). For each sample investigated the transition temperature and the latent heat of transition were determined in the way described below. The results are given in table 3. The numerical data differ slightly from the ones given by Franck (1961) because of the corrections made to the temperature scale as described in § 2·2 and because of an error regarding the pressure unit in that paper.

TABLE 3. PROPERTIES OF THE h.c.p.–f.c.c. TRANSITION IN ^{3}He AND ^{4}He

sample	$T_{tr.}$ (°K)	L (cal/mole)	$p_{tr.}$ (Kg/cm^2)	ΔS (cal mole^{-1} deg^{-1})	ΔV (cm^3/mole)
no. 1, ^{3}He T_m = 17·964 °K p_m = 1631·5 Kg/cm^2 V = 11·70 cm^3/mole	17·818	0·068	1629·1	0·0038	$1{\cdot}4 \times 10^{-4}$
no. 2, ^{3}He T_m = 18·688 °K p_m = 1730·7 Kg/cm^2 V = 11·56 cm^3/mole	17·896	0·067	1717·5	0·0037	$1{\cdot}4 \times 10^{-4}$
no. 3, ^{4}He T_m = 16·419 °K p_m = 1327·4 Kg/cm^2 V = 11·77 cm^3/mole	15·010	0·060*	1305·7	0·005†	4×10^{-4}†

* ΔE. † Data from Dugdale & Simon (1953).

The transition temperature was obtained from heating curves at constant energy input which showed a pronounced kink. The transition temperature was taken at the point where the heating curve first deviates from a straight line. Because of thermal and instrumental relaxation it was not possible to observe the natural width of the transition. The latent heat was obtained by making measurements of the apparent specific heat C_v^*, for a temperature interval that included the complete transition. As it was observed that the specific

heat, C_v, below and above the transition forms a continuous curve within the experimental scatter of about 1 % the excess energy consumption of the transition could be calculated from

$$\Delta E = (C_v^* - C_v)\,\Delta T$$

where ΔT is the temperature interval for which C_v^* had been measured and C_v is the interpolated specific heat at the centre of the heating interval. Within the experimental accuracy different heating intervals led to the same values of ΔE. This proves that the observed C_v^* data correspond to a real transition. The latent heat, L, of a transition is defined as the enthalpy change for the transition at constant pressure. As ΔE has been observed at constant volume a correction has to be applied to obtain L. This correction to ΔE turns out to be small for both ^{3}He and ^{4}He so that ΔE can be taken as virtually L. In table 3 we include values of the transition entropy $\Delta S = L/T$ and of the volume change ΔV calculated from the Clausius–Clapeyron equation.

The pressure at the transition temperature could be obtained from the pressure at the beginning of melting (as calculated from the data of Mills & Grilly) by the relation

$$p_{\mathrm{tr.}} - p_m = \int_{T_m}^{T_{\mathrm{tr.}}} (\delta p/\delta T)_v \,\mathrm{d}T = \int_{T_m}^{T_{\mathrm{tr.}}} (\delta S/\delta V)_T \,\mathrm{d}T. \tag{3}$$

For ^{3}He we obtain the phase separation line as

$$p_{\mathrm{tr.}} = 1609 + 1133(T - 17{\cdot}80)\ \mathrm{Kg/cm^2}, \tag{4}$$

where the triple point is at $T = 17{\cdot}80$ °K. It has been assumed here that the phase line is linear.

3·4. *The fluid range*

Measurements in the fluid range were extended up to 29 °K. The results for some selected molar volumes are included in figures 5 and 6. Smooth curves have been drawn through the experimental points and values of C_v read from these curves are given at rounded temperatures in tables 4 and 5. The scatter in the fluid range is much more pronounced

TABLE 4. SPECIFIC HEAT OF FLUID ^{4}He AT ROUNDED VALUES OF TEMPERATURE

	V = 16·25	14·55	12·22	11·77
T (°K)	C_v	C_v	C_v	C_v
7	1·84	—	—	—
8	1·99	—	—	—
9	2·13	—	—	—
10	2·25	2·12	—	—
11	2·36	2·22	—	—
12	2·47	2·32	—	—
13	2·56	2·42	—	—
14	2·65	2·51	—	—
15	2·72	2·59	—	—
16	2·79	2·67	—	—
17	2·85	2·75	—	—
18	2·90	2·81	2·64	—
19	2·93	2·87	2·72	—
21	2·99	2·98	2·85	2·79
23	3·02	3·05	2·95	2·90
25	3·04	3·10	3·04	3·00
27	3·04	3·12	3·11	3·09
29	3·04	3·13	3·16	3·16

Units: V (cm^3/mole); C_v (cal mole^{-1} deg^{-1}).

than in the solid range. This is probably due to the fact that in the liquid range the high-pressure capillaries connected to the calorimeter are filled with fluid up to a certain point beyond the adiabatic shield and this point will be temperature-dependent. It is therefore possible that a heat and mass transport through convection currents within the capillaries takes place. The volume of the capillaries up to the point where they are thermally anchored to the liquid helium can is about 0·005 cm³ as compared to 1·46 cm³ of the high pressure cell. It appears therefore that a mass transport alone would not seriously distort the results. The accompanying heat transport, however, could have such an effect. The accuracy can probably be estimated from the experimental scatter which is about 4%.

TABLE 5. SPECIFIC HEAT OF FLUID ^{3}He AT ROUNDED VALUES OF TEMPERATURE

	V =	17·02	16·87	15·72	14·98	14·16	14·11	13·56	13·33	12·57
T (°K)		C_v	C_v	C_v	C_v	C_v	C_v	C_v	C_v	C_v
6		1·38	1·40	—	—	—	—	—	—	—
7		1·56	1·55	—	—	—	—	—	—	—
8		1·72	1·70	1·62	—	—	—	—	—	—
9		1·86	1·84	1·75	—	—	—	—	—	—
10		1·99	1·97	1·88	1·83	—	—	—	—	—
11		2·11	2·09	2·00	1·94	1·90	1·90	—	—	—
12		2·22	2·20	2·11	2·04	1·99	1·99	—	—	—
13		2·31	2·30	2·21	2·14	2·08	2·07	2·04	—	—
14		2·40	2·38	2·30	2·23	2·16	2·16	2·12	2·09	—
15		2·48	2·46	2·38	2·32	2·24	2·24	2·19	2·17	—
16		2·55	2·54	2·45	2·40	2·32	2·32	2·27	2·26	—
17		2·61	2·61	2·53	2·47	2·40	2·40	2·34	2·34	2·28
18		2·66	2·67	2·60	2·54	2·46	2·47	2·41	2·41	2·34
19		2·72	2·72	2·66	2·61	2·53	2·54	2·48	2·48	2·40
21		2·82	2·81	2·77	2·72	2·65	2·66	2·61	2·61	2·51
23		2·90	2·89	2·86	2·81	2·76	2·76	2·72	2·72	2·62
25		2·98	2·94	2·92	2·88	2·85	2·84	2·81	2·80	2·73
27		—	2·99	2·98	2·93	2·92	2·90	2·89	2·87	2·82
29		—	3·03	3·03	2·97	2·97	2·97	2·95	2·93	2·90

Units: V (cm³/mole); C_v (cal mole^{-1} deg^{-1}).

3·5. *The thermal energy and entropy*

The thermal internal energy, $U-U_0$, and the lattice entropy, S, were calculated from the smoothed experimental data by means of the relation

$$U-U_0=\int_0^T C_v\,\mathrm{d}T \tag{5}$$

$$S=\int_0^T \frac{C_v}{T}\,\mathrm{d}T. \tag{6}\dagger$$

Here U_0 is the internal energy of the solid at 0 °K at the specified volume.

Values of $U-U_0$ and S for the solid at rounded values of temperatures are included in tables 1 and 2. Diagrams of the entropy over the whole temperature range investigated are given in figures 9 and 10. The melting entropy (at constant temperature), S_m, can be obtained from these figures and is plotted separately in figures 11 and 12. A comparison is made with the data of the melting entropy given by Grilly & Mills (1959) (obtained from

† In ^{3}He we are assuming that the nuclear spins are completely random in orientation so that for all the temperatures and densities considered here there is an additional constant term in the entropy of ^{3}He of magnitude $R\ln 2$ (cf. discussion on p. 11).

melting curve data by means of the Clausius–Clapeyron equation) and by Keesom & Keesom (1936) and Dugdale & Simon (1953) (from calorimetric data). It appears that the present data are from 1 to 2% lower than Grilly & Mills's data, but show the same temperature-dependence. This deviation is probably within the combined limit of error. The agreement with the earlier data of Keesom & Keesom, and of Dugdale & Simon is not so close.

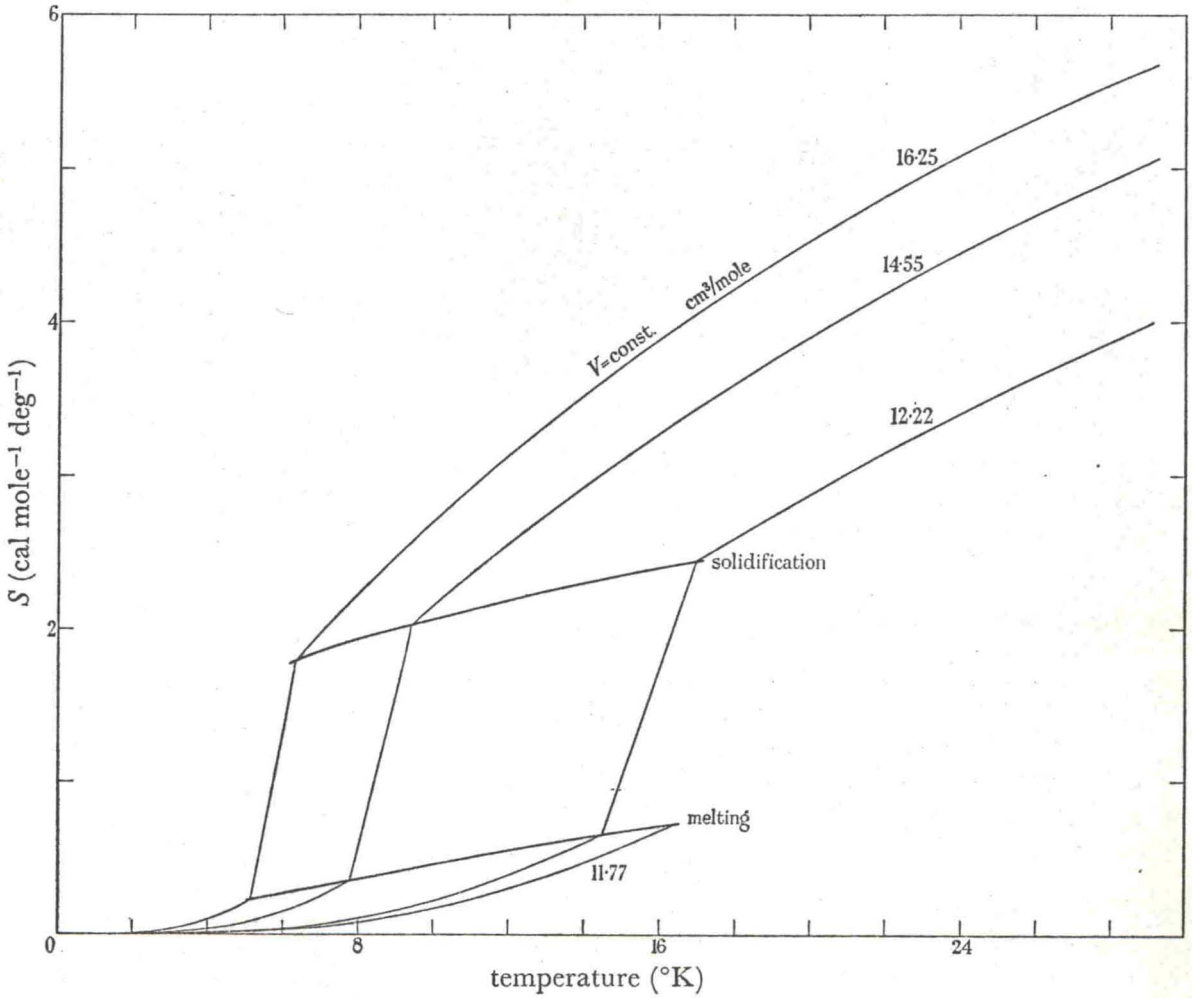

FIGURE 9. The entropy of ^{4}He. The numbered lines are lines of constant volume.

3·6. *Calculation of related thermodynamic properties*

The results given in the previous sections were derived by using the present experimental information only. A complete thermodynamic description, however, cannot be obtained from specific heat data alone. In addition to this one p-V-T relation over the experimental range covered has to be known. For this relation we took the melting curve, p against T and V against T as given by Mills & Grilly (1955), and Grilly & Mills (1959).

3·6·1. *Isochores and isotherms of solid* ^{4}He *and* ^{3}He

According to one of the Maxwell thermodynamic relations

$$(\partial S/\partial V)_T = (\partial p/\partial T)_V. \tag{7}$$

$(\partial S/\partial V)_T$ can be obtained from the experimental results by numerical differentiation. By using Mills & Grilly's p-V-T data and equation (7) we can then obtain the pressure at constant molar volume as a function of temperature, i.e. the isochores

$$p(T) = p_m - \int_T^{T_m} (\partial S/\partial V)_T \mathrm{d}T, \tag{8}$$

$$p_m = p(T_m), \quad V = \text{const.}$$

The isochores are given in tables 6 and 7 for rounded values of the molar volume. The columns of these tables give immediately the isotherms, i.e. $p = p(V)$ at constant temperature.

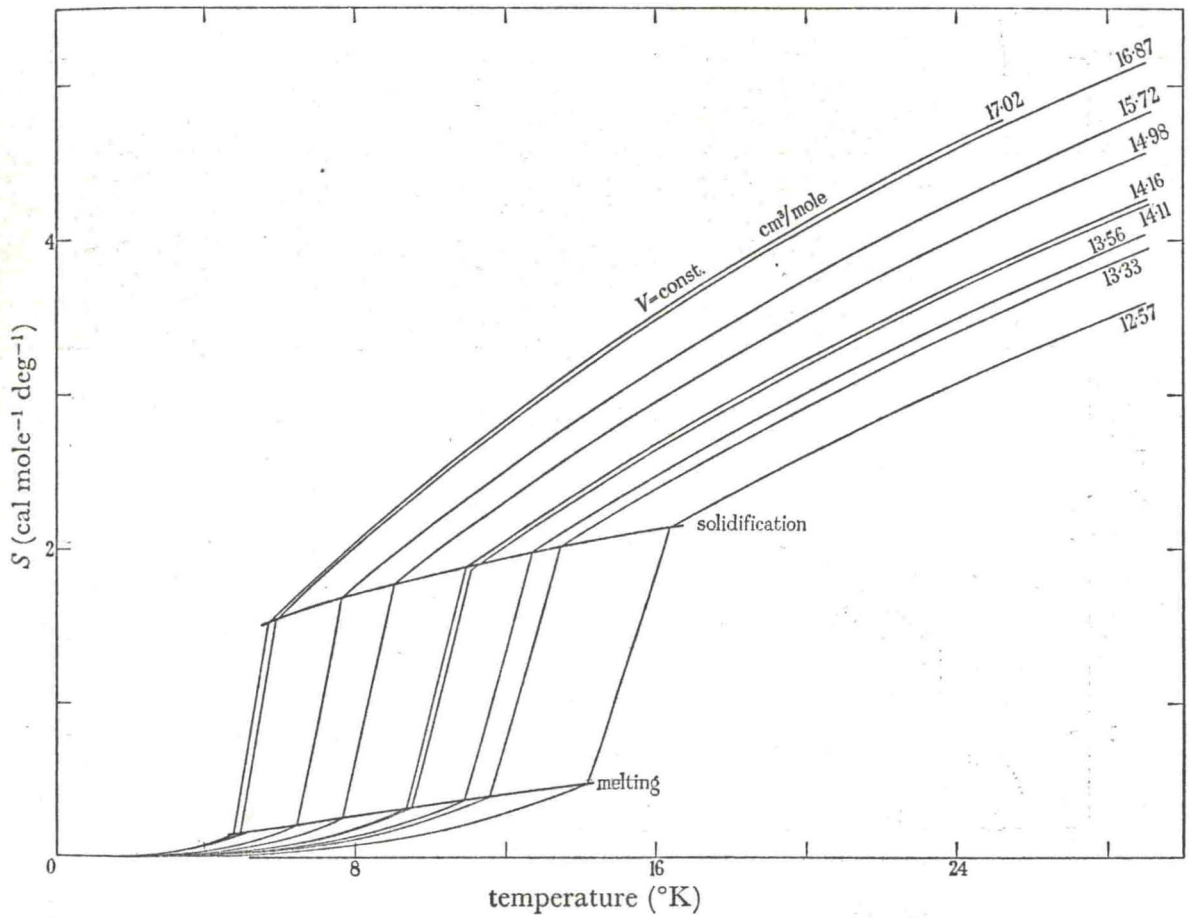

FIGURE 10. The lattice entropy of ^{3}He. The numbered lines are lines of constant volume.

3·6·2. *Compressibility*

We have calculated the compressibility of solid ^{4}He and ^{3}He at 0 °K from the 0 °K isotherm

$$\beta = -\frac{1}{V}\left(\frac{\partial V}{\partial p}\right)_{T=0}. \tag{9}$$

β is given at rounded values of molar volume in table 8.

3·6·3. *Thermal expansion coefficient*

The volume thermal expansion coefficient, α, can be obtained from the thermodynamical relation

$$\alpha = \beta(\partial p/\partial T)_V. \tag{10}$$

α for solid ^{4}He and ^{3}He is given as a function of temperature and molar volume in table 9.

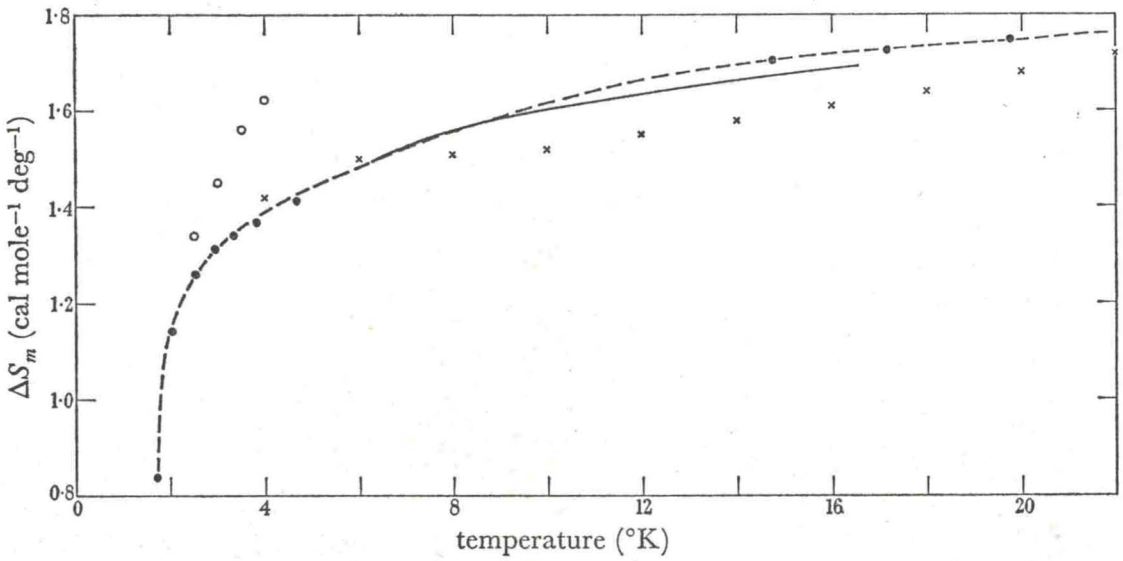

FIGURE 11. The melting entropy of ^{4}He as a function of temperature. ——, This work; --●--●, Grilly & Mills (1959); ×, Dugdale & Simon (1953); ○, Keesom & Keesom (1936).

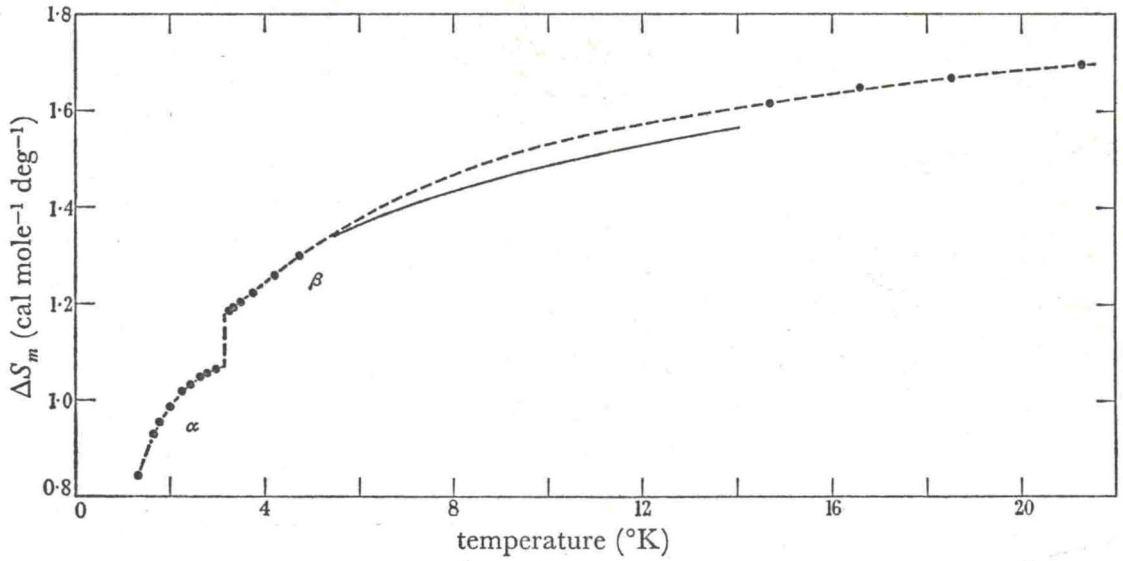

FIGURE 12. The melting entropy of ^{3}He as a function of temperature. ——, This work; --●--●, Grilly & Mills (1959).

TABLE 6. ISOCHORES FOR SOLID ^{4}He

	T = 0	2	4	6	8	10	12	14	15
V	p	p	p	p	p	p	p	p	p
12·0	1134·6	1134·6	1134·8	1135·9	1139·1	1146·2	1158·4	1178·2	1191·9
12·5	904·7	904·7	905·0	906·4	910·5	919·2	934·3	—	—
13·0	732·5	732·5	732·9	734·7	740·0	751·4	—	—	—
13·5	596·6	596·6	597·1	599·4	606·2	622·1	—	—	—
14·0	487·1	487·1	487·8	490·8	499·7	—	—	—	—
14·5	395·9	396·0	396·8	400·8	—	—	—	—	—
15·0	323·8	323·9	324·9	330·0	—	—	—	—	—
15·5	266·0	266·1	267·4	274·0	—	—	—	—	—
16·0	215·7	215·8	217·7	—	—	—	—	—	—
16·5	175·6	175·8	178·2	—	—	—	—	—	—

Units: T (°K); V (cm^3/mole); p (Kg/cm^2).

TABLE 7. ISOCHORES FOR SOLID ^{3}He

T = 0		2	4	6	8	10	12	14
V	p	p	p	p	p	p	p	p
12·5	1128·8	1128·8	1129·0	1129·7	1132·4	1138·7	1150·2	1167·6
13·0	931·7	931·7	931·9	932·9	936·1	943·4	956·5	—
13·5	772·9	773·0	773·3	774·6	778·8	787·8	—	—
14·0	644·1	644·2	644·6	646·3	651·7	—	—	—
14·5	538·9	539·0	539·4	541·8	548·7	—	—	—
15·0	453·7	453·8	454·4	457·4	—	—	—	—
15·5	383·7	383·8	384·6	388·5	—	—	—	—
16·0	326·4	326·5	327·4	—	—	—	—	—
16·5	278·3	278·4	279·7	—	—	—	—	—
17·0	238·0	238·1	239·7	—	—	—	—	—

Units: T (°K); V (cm^3/mole); p (Kg/cm^2).

TABLE 8. COMPRESSIBILITY OF SOLID ^{4}He and ^{3}He AT 0 °K

	$10^5\beta$ (cm^2/Kg)	
V (cm^3/mole)	^{4}He	^{3}He
12·0	15·9	—
12·5	20·0	18·3
13·0	24·8	21·8
13·5	30·0	26·0
14·0	36·0	30·8
14·5	43·1	36·4
15·0	51·2	43·0
15·5	59·9	51·0
16·0	70·1	60·0
16·5	—	69·4
17·0	—	79·6

TABLE 9. VOLUMETRIC THERMAL EXPANSION COEFFICIENT OF SOLID ^{4}He AND ^{3}He

	$10^3\alpha$ (deg^{-1})						
V	T = 2	4	6	8	10	12	14
			^{4}He				
12	0·004	0·037	0·151	0·39	0·78	1·35	2·20
13	0·009	0·101	0·40	0·98	2·02	—	—
14	0·030	0·260	0·94	2·54	—	—	—
15	0·070	0·60	2·32	—	—	—	—
16	0·156	1·38	—	—	—	—	—
			^{3}He				
13	0·009	0·049	0·198	0·54	1·10	1·94	
14	0·018	0·127	0·49	1·27	—	—	
15	0·037	0·285	1·17	—	—	—	
16	0·082	0·63	2·67	—	—	—	
17	0·149	1·56	—	—	—	—	

Units: T (°K); V (cm^3/mole).

3·6·4. *The internal energy at* 0 °K

In all subsequent discussion, the zero of energy will be taken as that of the infinitely separated atoms with zero kinetic energy (i.e. at 0 °K). With this zero of energy the experimental value of the internal energy at 0 °K and volume V can be obtained from the relation

$$U_0 = -L_0 - \int_{V_1}^{V_2} p\,\mathrm{d}V + p_m \Delta V_m - \int_{V_3}^{V} p\,\mathrm{d}V. \qquad (11)$$

L_0 is the latent heat of vaporization at 0 °K, $p_m \Delta V_m$ is the work done in solidifying the liquid at 0 °K, and the two integrals give the work of compression in the liquid and the solid range, respectively. (V_1 is the volume of the liquid in equilibrium with its vapour, V_2 in equilibrium with the solid, and V_3 that of the solid in equilibrium with the liquid.)

TABLE 10

	p (Kg/cm²)	V (cm³/mole)	U_0 (cal/mole)
liquid 0 °K	0	36·63	−5·04
liquid 0 °K	29	26·0	−2·6
b.c.c. solid 0 °K	29	24·2	−1·8

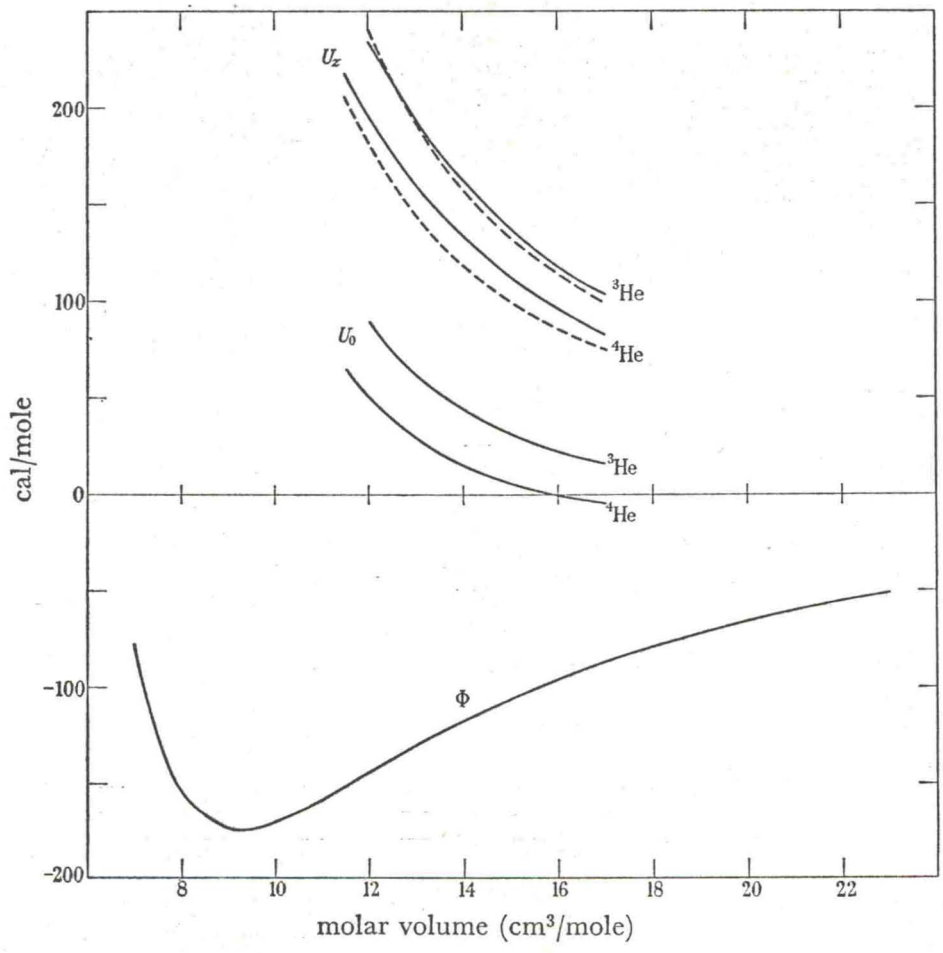

FIGURE 13. Energy relations at 0 °K for solid ^{4}He and ^{3}He. U_z is the zero-point energy; U_0 is the internal energy at absolute zero; and Φ is the classical static lattice energy calculated from the de Boer–Michels potential. ——, Experimental; ------, London (1954).

For ^{4}He we have taken Swenson's (1950) estimate for one value of U_0. According to this, U_0 for the solid at the melting pressure is −11·9 cal/mole. In order to obtain U_0 for smaller molar volumes we have to calculate the work of compression according to equation (11). This information is known from the present experiments between 17·0 and 11·5 cm³/mole. Up to $V = 17$ cm³/mole we have used an extrapolation of the isotherm at 0 °K. This extrapolation gives $U_0 = -5{\cdot}07$ cal/mole for $V = 17{\cdot}0$ cm³/mole.

The calculation of U_0 in the case of ^{3}He is complicated by the fact that ordering of the nuclear spins starts in the *liquid phase* below roughly 1 °K. We have tried to eliminate this effect by extrapolating the various quantities from above 1 °K towards 0 °K. The thermal energy associated with complete spin ordering is, however, certainly less than 1 cal/mole and is therefore not important for the present purpose.

From the vapour pressure data of Sydoriak & Roberts (1957) we find $L_0 = -5{\cdot}04$ cal/mole for liquid ^{3}He at zero pressure. The work of compression of the liquid up to the melting pressure was estimated from the data of Sherman & Edeskuty (1960); this gives 2·5 cal/mole. The change in U_0 upon solidification was estimated as 0·8 cal/mole from the results of Mills, Grilly & Sydoriak (1961), and of Grilly & Mills (1959). The melting pressure at 0 °K was taken as 29 Kg/cm^2. Table 10 gives the different steps of the calculation. The work of compression up to $V = 16{\cdot}5$ cm^3/mole, the lowest part of the 0 °K isotherm known experimentally was estimated at 20·5 cal/mole. For this we used, as in the case of ^{4}He, an extrapolation of the 0 °K isotherm taking the melting line of Grilly & Mills (1959) as a guide. This procedure is reliable to probably better than 1 cal/mole because the 0 °K isotherm is quite close to the melting line in this density range. The transition, from b.c.c. ^{3}He to h.c.p ^{3}He, which was estimated by Mills & Grilly (1959) to have zero volume change at 0 °K, has been neglected.

Values of U_0 for both isotopes are shown as a function of volume in figure 13.

4. Discussion

4·1. *The specific heat of solid helium*

At temperatures sufficiently low that the wavelengths of the excited lattice vibrations are long compared to the interatomic distance, the continuum model should describe the behaviour of the actual solid very accurately and C_v should be given by the well-known relation

$$C_v = \frac{12\pi^4}{5} R \left(\frac{T}{\theta_0}\right)^3. \tag{11}$$

Here R is the gas constant and θ_0 the limiting low-temperature value of the Debye temperature which can also be calculated from the low-temperature elastic constants of the solid (cf. Barron & Klein 1962). This T^3 behaviour is to be expected only at temperatures below about $\theta/50$. Above this θ_D will in general be temperature dependent; figure 14 illustrates the kind of temperature dependence to be expected of θ_D for a harmonic solid with short-range forces and a close-packed structure. At high temperatures θ_D would, in this model, again become constant at a value usually referred to as θ_∞.

For solid ^{3}He and ^{4}He we see (from figures 7 and 8) the fall in θ_D with increasing temperature but no minimum in the curve. This may be because melting and 'pre-melting' (perhaps the onset of vacancy formation) prevent us from seeing this part of the curve at these densities. The magnitude of the change in θ_D with temperature is, however, not very different from that found in other inert gas solids such as argon and krypton over the corresponding range of temperatures (cf. Beaumont, Chihara & Morrison 1961).

If at these densities solid helium approximated to a harmonic solid, the values of θ_D at lower temperatures would be similar to those indicated by the dashed lines in figures 7 and 8.

The experimental data from 0·3 to 1·5 °K due to Heltemes & Swenson (1962) do not, however, confirm these expectations. According to their measurements, the specific heats of both isotopes tend to be higher than those corresponding to the dashed lines in figures 7 and 8; in fact Heltemes & Swenson conclude that there is, in addition to the term in $(T/\theta)^3$, an additional contribution to the specific heat approximately proportional to T. This contribution does not change much with volume and is of similar magnitude in both ^{3}He and ^{4}He. On the plot of θ_D against T this would show as a maximum in the curve for a particular density followed by a rather rapid fall in θ_D at the lowest temperatures. In the preliminary account of their experiments, Heltemes & Swenson (1961) assumed that this linear term was spurious and due to some unexplained peculiarity of the apparatus. Since, however, they were subsequently unable to find anything wrong with the apparatus, it is not

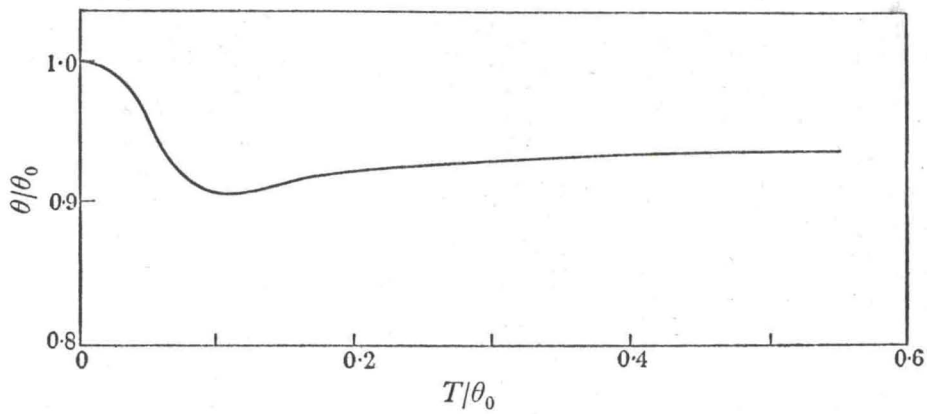

FIGURE 14. The dependence of θ_D on temperature as calculated for an f.c.c. lattice (after Leighton 1948). The precise form of the curve depends on the force constants chosen.

at present clear whether this contribution to the specific heat is a genuine effect or not. The situation clearly calls for better data, especially in the range 1 to 4 °K, to obtain more reliable information on the temperature variation of θ_D in this range. This uncertainty means that we cannot convincingly extrapolate the θ_D curves to 0 °K. Although this is unfortunate in that we cannot then evaluate θ_0, it does not appreciably affect the calculations of the entropy and internal energy of the solid already described, since the contribution to these quantities from this small term in the specific heat is negligible.†

Since reliable values of the Debye temperature at 0 °K cannot be obtained at present, we base the following discussion of the volume dependence of θ_D on a comparison at constant reduced temperature (i.e. at constant T/θ_D). The lowest reduced temperature for which experimental values of θ_D were obtained is $T/\theta_D = \frac{1}{18}$. In figure 15 we have plotted θ_D as function of molar volume for $T/\theta_D = \frac{1}{18}$. From these curves we can derive a value for the Gruneisen constant γ

$$\gamma = -\partial \ln \theta / \partial \ln V. \tag{12}$$

We find for both isotopes almost independent of molar volume $\gamma = 2{\cdot}4$.

† [*Note added in proof*, 10 *June* 1964.] Recent measurements (Franck, to be published) from 1·3 to 4 °K on solid ^{4}He for molar volumes between 10·85 and 16·30 cm^3/mole have shown an anomalous linear term in the specific heat similar to that found by Heltemes & Swenson. The extrapolated Debye temperature at 0 °K agrees with the data reported by Heltemes & Swenson if the anomalous linear term is neglected in both sets of measurements. The nature of the anomaly is not clear at present. There are indications, however, that the anomaly is much reduced (to roughly 1/3) in well-annealed samples.

We have also compared the Debye temperatures for different molar volumes as a function of the reduced temperature T/θ_D. This comparison is made in table 11 where values of $\theta_D(V)/\theta_D(V_0)$ are listed as functions of T/θ_D (we chose $V_0 = 12{\cdot}57$ cm³/mole for ³He and

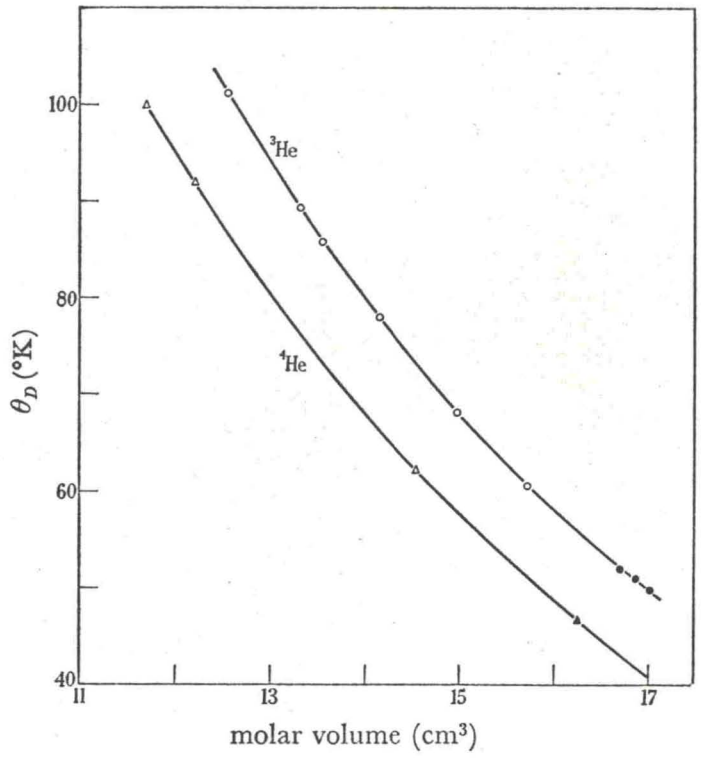

FIGURE 15. The Debye temperatures of solid ⁴He and solid ³He as a function of volume at the same reduced temperature ($\theta_D/T = 18$). The open points are directly measured values; the closed points are extrapolated from a slightly higher reduced temperature.

TABLE 11. $\theta_D(V)/\theta_D(V_0)$ AT DIFFERENT REDUCED TEMPERATURES FOR SOLID ³He AND SOLID ⁴He

(V_0 has been taken as 12·57 cm³ mole for ³He and 11·77 cm³ mole for ⁴He)

V (cm³) =	13·33	13·56	14·16	14·98	15·72	16·71	16·87	17·02
θ/T				³He				
18·0	0·881	0·846	0·769	0·672	0·597	—	—	—
15·2	0·874	0·844	0·767	0·671	0·601	0·514	0·504	0·490
12·9	0·875	0·841	0·761	0·668	0·596	0·513	0·503	0·491
11·0	0·872	0·837	0·761	0·667	0·594	0·509	0·499	0·488
9·7	0·874	0·840	0·758	0·664	0·590	0·501	0·493	0·480
8·25	0·874	0·839	0·756	0·656	—	—	—	—

V (cm³) =	12·22	14·55	16·25
θ/T		⁴He	
18·0	0·919	0·620	—
12·0	0·923	0·624	0·474
9·0	0·920	0·614	0·462

$V_0 = 11{\cdot}77$ cm³/mole for ⁴He). There is clearly a systematic change in this ratio as the melting point is approached. This might be due, for example, either to anharmonic effects in the lattice vibrations or to the formation of vacancies in the lattice. Apart from this

range, the ratio seems to be almost constant. This implies therefore that there exists to a good approximation a reduced θ_D curve of the form

$$\theta_D = F(V)f(T/\theta_D). \tag{13}$$

Since $-\partial \ln \theta / \partial \ln V = 2{\cdot}4$ and is very nearly constant over the whole volume range investigated, we can write $F(V) \propto V^{-2{\cdot}4}$. These results mean that a Gruneisen equation of state describes the data quite well over a wide range of volumes and temperatures.

As already mentioned, it should be possible to calculate values of θ_0 from the elastic constants of the solid at the density of interest. Although we do not know the complete elastic constants of solid helium we do know its compressibility as a function of volume. From this alone it is possible to calculate an approximate value of θ_0 by making some assumption about how Poisson's ratio varies with volume. The simplest relation of this kind implies that

$$\theta \propto (a/\beta m)^{\frac{1}{2}}, \tag{14}$$

where a is the lattice parameter, β the compressibility, and m the mass of the atom. In table 12 we compare the experimental values of θ_D evaluated at the same reduced temperature ($\theta_D/T = 18$) with the corresponding values of $(a/\beta m)^{\frac{1}{2}}$ for both helium isotopes.

TABLE 12. COMPARISON OF θ_D FROM SPECIFIC HEATS WITH θ ESTIMATED FROM THE COMPRESSIBILITY

The values of θ_D are taken at the same reduced temperature $T/\theta_D = 18$. The values in brackets are extrapolated from slightly higher reduced temperatures.

V (cm³/mole)	θ_D (°K)	$\theta_D(\beta m/V^{\frac{1}{3}})^{\frac{1}{2}}$
	^{3}He	
12·57	101·2	500
13·33	89·3	497
13·56	85·8	496
14·16	78·0	495
14·98	68·1	491
15·72	60·5	491
16·71	(51·9)	482
16·87	(50·9)	483
17·02	(49·6)	480
	^{4}He	
11·77	99·9	499
12·22	91·9	509
14·55	62·0	526
16·25	(46·6)	510

(Instead of a, the lattice parameter, we have written $V^{\frac{1}{3}}$.) The last column of the table gives the product $\theta_D(\beta m/V^{\frac{1}{3}})^{\frac{1}{2}}$. Although for ^{3}He it shows small systematic changes and for ^{4}He some bigger, apparently random, changes, this product remains rather constant over the whole range. We may therefore conclude that the volume dependence of θ reflects quite closely the volume dependence of β. By putting in a reasonable value for the constant of proportionality in equation (14) (cf., for example, Mitra & Joshi 1961) it is found that the magnitude of θ so calculated is similar to the values of θ_0 indicated by the extrapolations in figures 7 and 8. Since the theory is only approximate this agreement is not very significant but it does perhaps suggest that if there is a low temperature anomalous contribution to the specific heat as found by Heltemes & Swenson it is *not* due to the lattice vibrations.

4·2. *Energy relations in solid helium at* 0 °K

For the interaction between two helium atoms we assume the de Boer–Michels potential† (de Boer & Michels 1938)

$$\phi = (Br^{-12} - Cr^{-6})\, 10^{-12}\,\text{erg}, \tag{15}$$

where $B = 447$, $C = 1{\cdot}59$, and r, the distance between the centres of both atoms, is measured in ångströms. We further assume that the energy in a system of many atoms can be calculated by simply superimposing the two-body potential of equation (15). In order to define the *static* lattice energy, Φ, we assume that the atoms are held rigidly at their average positions (the lattice sites). The energy Φ can then be calculated from equation (15) by taking account of all interactions:

$$\Phi = \tfrac{1}{2} \sum_{i \neq j} \phi(r_{ij}), \tag{16}$$

where the sum extends over all lattice sites. According to quantum theory this is not the ground state. In classical terms we can say that even at 0 °K the atoms vibrate around their average positions. This can be seen as a consequence of the uncertainty principle. Owing to this zero-point motion the internal energy at 0 °K, U_0, is higher than the static lattice energy, and the difference between these energies is defined as zero-point energy U_z,

$$U_z = U_0 - \Phi. \tag{17}$$

(In this relation, all the quantities depend on volume.)

Because the definition of U_z involves Φ, which can be only obtained through consideration of a hypothetical classical model of the solid, the zero-point energy cannot be determined directly from experiment. The concept of zero-point energy is, however, valuable because it provides a convenient measure of the influence of quantum corrections.

In figure 13 we have given the static lattice potential, Φ, calculated from the de Boer–Michels potential (equation (15)), the internal energy, U_0, at 0 °K for solid ^{4}He and ^{3}He, and the zero-point energy U_z, for both isotopes. It will be noticed that U_0 is positive over most of the volume range of our experiments.

Several calculations of the ground state of solid helium have been published. London (1954) and Hurst & Levelt (1961) used a cell model of the solid. London considered a spherical rigid box, whereas Hurst & Levelt used a sphericalized potential derived from the actual interatomic potential and the observed lattice structure. The cell model is essentially a one-particle model and corresponds to the Einstein approximation in the theory of specific heats.

Quantum-mechanical variational methods have been used by Bernardes (1960), by Saunders (1962), and by Nosanow & Shaw (1962) to obtain an estimate of the energy of the ground state of solid helium. Nosanow & Shaw review the previous variational treatments and conclude that such a method using spherically symmetric, single-particle wave functions is not adequate for calculating the ground states of solid ^{3}He or ^{4}He.

† We have chosen this version of the helium interatomic potential because it is derived from low-temperature gas data; these data emphasize the low energy part of the potential curve, which is important here. For a more detailed discussion see Hooton (1955).

In figure 13 we give a comparison of the experimental value of U_z with the calculations of London (1954); it can be seen that the volume dependence of U_z is reasonably well reproduced by this theoretical expression. It must, however, be borne in mind that the uncertainty in the experimental value of U_z is large, mainly because of uncertainties in the interatomic potential used to calculate Φ. By comparing the de Boer–Michels potential with other proposed potentials (Yntema & Schneider 1950; Slater & Kirkwood 1931) one finds that uncertainties of up to 15% exist due to this cause. Therefore the rather good agreement of London's calculations with the experimental results is partly fortuitous.

A different approach to the calculation of the zero-point energy is through the vibrational properties of the lattice. Domb & Salter (1952) showed that at least for cubic Bravais lattices and harmonic oscillations the zero-point energy is given very closely by

$$U_z = \tfrac{9}{8}R\theta_\infty, \tag{18}$$

where θ_∞ is the (theoretical) high-temperature limit of the Debye temperature. Salter (1954) has used this expression for the discussion of the zero-point properties of the heavier rare gas solids. No satisfactory theoretical derivation of equation (18) has been given for the case of helium where the zero-point vibrations are strongly anharmonic. Nevertheless, our results on helium show that U_z is proportional to θ_D for both isotopes (θ_D is again evaluated at the same reduced temperature for all densities in both isotopes). They show further that the constant of proportionality is about that to be expected from equation (18) if one estimates θ_∞ from the low-temperature part of the curve of θ_D against T. It is thus probable from the evidence of the present experiments that even in this extreme case, equation (18) still describes the experimental results surprisingly well.

Although the large amplitude of the zero-point motion in solid helium introduces many difficulties into the calculation of U_0 at low densities, it is to be expected that as the density increases (volume decreases) the zero-point energy will become less and less important in comparison with the energy associated with the repulsive forces between the atoms. (U_z varies approximately as V^{-2} (since $\gamma \simeq 2$) whereas the potential of the repulsive forces varies as something like V^{-4}.) At small enough volumes, therefore, we may expect that the ratio of the values of U_0 for both isotopes will tend towards unity. Similarly, the restoring forces produced when the lattice is perturbed will tend to become the same in the two isotopes so that the frequencies of the resulting vibrations will be determined by the ratio of the masses of the two kinds of atoms, i.e. the ratio θ_3/θ_4 will tend to the limiting value $(m_4/m_3)^{\frac{1}{2}}$ as the volume is diminished, provided that no changes in the electronic band structure of the solids intervene.

In table 13 we give the ratio of the Debye temperatures for ^{3}He and ^{4}He, compared at the same molar volume and at the same reduced temperature, in units of $(m_4/m_3)^{\frac{1}{2}}$. The ratio of the Debye θ's measured at the same reduced temperature varies very little with temperature so that this comparison can be made quite accurately. It can be seen that the ratio of the Debye temperatures tends towards $(m_4/m_3)^{\frac{1}{2}}$ at low molar volumes. At high molar volumes, this ratio is exceeded by up to 7%. This is qualitatively in accordance with perturbation anharmonic theory which shows that when anharmonic effects come in, the θ of the lighter isotope (in which therefore the anharmonic effects are greater) will increase more rapidly than that of the heavier isotope (T. H. K. Barron, private communication).

TABLE 13. COMPARISON OF THE DEBYE TEMPERATURES OF SOLID ^{3}He AND ^{4}He AS A FUNCTION OF VOLUME

V (cm^3/mole)	$(m_3/m_4)^{\frac{1}{2}}\,\theta_3/\theta_4$
12·5	1·028
13	1·030
14	1·035
15	1·040
16	1·058
16·5	1·074

4·3. *The fluid helium isotopes*

Only a few experimental determinations of the specific heat of fluid helium at high density are reported. Eucken (1916) measured C_v at fairly low densities over the temperature range 16 to 32 °K. A few observations were reported by Keesom & Keesom (1936) and by Dugdale & Simon (1953). Hill & Lounasmaa (1960) covered the range up to a pressure of 100 Kg/cm^2, corresponding to $V = 19{\cdot}4$ cm^3/mole from 1·2 to 4 °K. The results of Hill & Lounasmaa do not overlap with the present set of measurements; they seem, however, to form a reasonable extrapolation.

The characteristic result of the present set of measurements is that C_v at the high temperature limit tends towards the value $\frac{3}{2}R$ (or slightly above this value) independent of the molar volume. At low temperatures C_v decreases in a monotonic way until the solidification point is reached. A close similarity exists between the behaviour of both isotopes and, in the range of densities and temperatures investigated, there seems to be no detectable influence of the different particle statistics.

The fall in C_v with falling temperature is thus *not* attributable to simple ideal gas degeneracy: it seems more probable that the fall-off is due to localized vibrations of the atoms of the fluid. Let us suppose that each atom is imprisoned in a cell formed by neighbouring atoms. At low energies, the energy levels available to the atoms will be discrete so that when kT falls to a value comparable with the energy difference between these levels, C_v will begin to diminish. At higher energies, the energy levels will be more like those of a free particle in a box. This model of a fluid, which was developed by Eucken and his co-workers (Eucken & Seekamp 1928; Bartholomé & Eucken 1937) and more recently by Levelt & Hurst (1960) has been applied with some success to the explanation of the temperature dependence of C_v in other simple fluids such as the hydrogen isotopes and the heavier inert gases. The model implies that C_v may rise above $\frac{3}{2}R$ (indeed in the extreme limit it may reach $3R$) before falling again at higher temperatures to the classical limit of $\frac{3}{2}R$, characteristic of monatomic gases. The actual temperature dependence of C_v is, of course, determined by the detailed form of the potential which is assumed to exist within the cell. Here, however, we wish only to point out that a model of this kind will explain not only the decrease of C_v at lower temperatures in the fluid helium isotopes but also why, in these fluids, C_v appears to rise above $\frac{3}{2}R$ at higher temperatures, as indicated in figures 5 and 6.

CONCLUSIONS

The behaviour of the specific heats of the solid helium isotopes at very low temperatures is still obscure. (But see the note added in proof on p. 22.) Until this has been convincingly established and understood, conclusions about their behaviour at higher temperatures must

be tentative. With this reservation we would draw the following conclusions from our experiments. As far as the close-packed phases are concerned, solid helium in both isotopic forms appears to behave normally, i.e. it can be understood at least semi-quantitatively in terms of existing theories and concepts. For example, the zero-point energy can be estimated roughly by means of a crude cell model due to London, or by means of a quasi-harmonic model of the vibrations of the solids. Likewise the temperature dependence of the specific heats appears to be similar to that of a quasi-harmonic close-packed solid and the magnitude of the characteristic temperature at each density agrees with what is known about the mechanical properties of the solids.

The specific heat of the fluid isotopes can be understood qualitatively; at present there appears to be no possibility of a detailed comparison with fundamental theory.

The authors gratefully acknowledge the encouragement and interest of the late Dr D. K. C. MacDonald, F.R.S. They are grateful to Dr T. H. K. Barron for many valuable discussions; to Dr D. L. Martin for general advice on calorimetry; to Dr Barron and Dr A. M. Guénault for reading the manuscript; and to Dr C. A. Swenson for communicating his results before publication. The authors also wish to thank Mr A. A. M. Croxon and Mr R. L. Snowdon for their valuable technical help; and Miss B. A. Cotton and Mr D. R. Taylor for their work on the calculations.

References

Barron, T. H. K. & Klein, M. L. 1962 *Phys. Rev.* **127**, 1997.
Bartholomé, E. & Eucken, A. 1937 *Trans. Faraday Soc.* **33**, 45.
Beaumont, R. H., Chihara, H. & Morrison, J. A. 1961 *Proc. Phys. Soc.* **78**, 1462.
Bernardes, N. 1960 *Phys. Rev.* **120**, 1927.
Bernardes, N. & Brewer, D. F. 1962 *Rev. Mod. Phys.* **34**, 190.
Clement, J. R. 1955 *Temperature, its measurement and control in science and industry*, vol. 2, p. 380. New York: Reinhold.
de Boer, J. & Michels, A. 1938 *Physica*, **5**, 945.
Domb, C. & Dugdale, J. S. 1957 *Progress in Low Temperature Physics*, vol. 2, p. 338. North Holland Publishing Company.
Domb, C. & Salter, L. 1952 *Phil. Mag.* **43**, 1083.
Dugdale, J. S. & Simon, F. E. 1953 *Proc. Roy. Soc.* A, **218**, 291.
Eucken, A. 1916 *Verh. dtsch. Phys. Ges.* **18**, 4.
Eucken, A. & Seekamp, H. 1928 *Z. phys. Chem.* **134**, 178.
Franck, J. P. 1961 *Phys. Rev. Lett.* **7**, 435.
Franck, J. P. & Martin, D. L. 1961 *Canad. J. Phys.* **39**, 1320.
Grilly, E. R. & Mills, R. L. 1959 *Ann. Phys.* **8**, 1.
Heltemes, E. C. & Swenson, C. A. 1961 *Phys. Rev. Lett.* **7**, 363.
Heltemes, E. C. & Swenson, C. A. 1962 *Phys. Rev.* **128**, 1512.
Hill, R. W. & Lounasmaa, O. V. 1960 *Phil. Trans.* A, **252**, 357.
Hooton, D. J. 1955 *Phil. Mag.* **46**, 422, 433, 485.
Hurst, R. P. & Levelt, J. M. H. 1961 *J. Chem. Phys.* **34**, 54.
Keesom, W. H. 1942 *Helium*, p. 42. Amsterdam: Elsevier.
Keesom, W. H. & Keesom, A. P. 1936 *Comm. Leiden*, no. 240*b*.
Leighton, R. B. 1948 *Rev. Mod. Phys.* **20**, 165.
Levelt, J. M. H. & Hurst, R. P. 1960 *J. Chem. Phys.* **32**, 96.
London, F. 1954 *Superfluids*, vol. 2. New York: Wiley.

Mills, R. L. & Grilly, E. R. 1955 *Phys. Rev.* **99**, 480.
Mills, R. L. & Schuch, A. F. 1961 *Phys. Rev. Lett.* **6**, 263.
Mills, R. L., Grilly, E. R. & Sydoriak, S. G. 1961 *Ann. Phys.* **12**, 41.
Mitra, S. S. & Joshi, S. K. 1961 *Physica*, **27**, 376.
Nosanow, H. L. & Shaw, G. L. 1962 *Phys. Rev.* **128**, 546.
Salter, L. 1954 *Phil. Mag.* **45**, 360.
Saunders, E. M. 1962 *Phys. Rev.* **126**, 1724.
Schuch, A. F. & Mills, R. L. 1961 *Phys. Rev. Lett.* **6**, 596.
Sherman, R. H. & Edeskuty, F. J. 1960 *Ann. Phys.* **9**, 522.
Simon, F. E. 1934 *Nature, Lond.* **133**, 529.
Slater, J. C. & Kirkwood, J. G. 1931 *Phys. Rev.* **37**, 682.
Swenson, C. A. 1950 *Phys. Rev.* **79**, 626.
Sydoriak, S. G. & Roberts, T. R. 1957 *Phys. Rev.* **106**, 175.
Yntema, J. L. & Schneider, W. G. 1950 *J. Chem. Phys.* **18**, 641.